UCRL-JC-123154
PREPRINT

CONF-9606229--6

Electron Density Measurement of a Colliding Plasma Using Soft X-Ray Laser Interferometry

A. S. Wan, C. A. Back, T. W. Barbee, Jr., R. Cauble P. Celliers
L. B. DaSilva, S. Glenzer, J.C. Moreno, P. W. Rambo, G. F. Stone,
J. E. Trebes and F. Weber

This paper was prepared for submittal to the
5th International Conference on X-ray Lasers
Lund, Sweden, June 10-14, 1996

May 1996

Lawrence Livermore National Laboratory

ELECTRON DENSITY MEASUREMENT OF A COLLIDING PLASMA USING SOFT X-RAY LASER INTERFEROMETRY

A. S. WAN, C. A. BACK, T. W. BARBEE, JR, R. CAUBLE, P. CELLIERS, L. B. DASILVA, S. GLENZER, J. C. MORENO, P. W. RAMBO, G. F. STONE, J. E. TREBES, F. WEBER

Lawrence Livermore National Laboratory, P. O. Box 808, Livermore CA 94550

The understanding of the collision and subsequent interaction of counter-streaming high-density plasmas is important for the design of indirectly-driven inertial confinement fusion (ICF) hohlraums. We have employed a soft x-ray Mach-Zehnder interferometer, using a Ne-like Y x-ray laser at 155 Å as the probe source, to study interpenetration and stagnation of two colliding plasmas. We observed a peaked density profile at the symmetry axis with a wide stagnation region with width of order 100 μm. We compare the measured density profile with density profiles calculated by the radiation hydrodynamic code LASNEX and a multi-specie fluid code which allows for interpenetration. The measured density profile falls in between the calculated profiles using collisionless and fluid approximations. By using different target materials and irradiation configurations, we can vary the collisionality of the plasma. We hope to use the soft x-ray laser interferometry as a mechanism to validate and benchmark our numerical codes used for the design and analysis of high-energy-density physics experiments.

1. Introduction

The understanding of the collision and subsequent interaction of counter-streaming high-density plasmas is important for the design of ICF hohlraums [1]. In a typical indirectly-driven vacuum hohlraum, the interaction of the optical laser drive with high-Z inner surfaces generates counter-streaming plasmas which flow unimpeded and collide on the axis of cylindrically-shaped hohlraums. Single-fluid radiation hydrodynamics codes that we typically use to design ICF and other laser-plasma experiments, such as LASNEX [2], do not allow for plasma interpenetration. Without interpenetration, as the plasmas collide and stagnate, their kinetic energy converts to internal energy, resulting in unphysically large ion temperature which generates strong shocks that propagate away from the axis of symmetry. Furthermore, as the plasma stagnate on the hohlraum axis, the single-fluid codes predict the creation of jets of high-velocity and high-density plasmas, which stream toward the capsule located at the center of the hohlraum and destroy the symmetry of the capsule implosion before capsule ignition. Current hohlraum designs for Nova [3,4,5] and the point design for the National Ignition Facility [1,5,6] employ a low-density fill gas to impede the plasma blowoff from stagnating on the hohlraum axis.

Past experimental studies of colliding plasmas have primarily focused on laser-produced, low-Z (Al, Si) front-illuminated thick targets [7,8,9,10] and back-illuminated exploding thin foils [11]. Most of the experiments utilizes x-ray spectroscopy and imaging techniques to characterize the plasma parameters, such as the measurement of T_e through line-ratio and ionization balance, T_i using line shape, and spatial and temporal images of the plasma collision using x-ray pinhole imaging. Bosch et al. [7] employed a holographic interferometer at 2630 Å to measure snapshots of the n_e profiles.

2. Experimental Setup, Results, and Data Analysis

Recent demonstration of soft x-ray interferometry is a significant step in the measurement of 2-D n_e profiles of high-density, fast-evolving, and large scale length laser-produced plasmas [12], and allows for us to examine the dynamics of colliding plasma in ICF-rele-

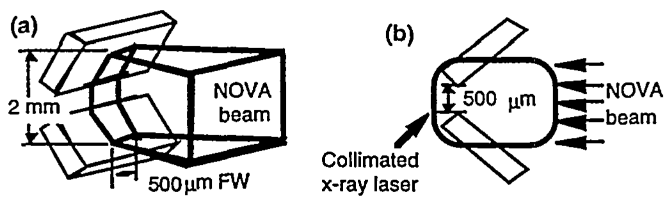

Fig. 1 The colliding plasma experimental setup. (a) 3-D view of Nova beam illuminating the 2 Au slabs. (b) side view showing the window of collimated x-ray laser beam which defines the view of the gated detector.

vant regime. Compare to conventional optical interferometers [7], we operate at 155 Å, using a collisionally pumped Ne-like Y x-ray laser as the probe source, which allows us to obtain a two order of magnitude enhancement in spatial resolution due to reduced light refraction and more than a three order of magnitude enhancement in signal strength because of reduced absorption. The short pulse and high brightness of the x-ray laser allowed us to obtain an interferogram in a single 350 ps exposure thereby reducing the effects of vibrations and motion blurring. The timing between the two Nova lasers, one to generate the x-ray laser and one to produce the target laser plasma, was defined by the time-of-flight path of our interferometer setup and the desired probe time.

The setup of our first colliding plasma experiment is shown in Fig. 1. Two Au slabs are aligned at 45 deg with respect to the symmetry axis. The minimum gap between the tips of the two slabs is 500 μm. We generate a 500 μm full-width line-focused laser beam which incidents the slabs, as shown in Fig. 1(a), and generates plasmas blowing toward each other. The laser has an intensity on target of 3×10^{14} W/cm^2 and has a 1-ns squared temporal pulse shape. At late time the two plasma streams collide at the symmetry axis. By varying the geometry, the slab materials, and the intensity of the incident laser, we can change the collisionality of the plasma. At high density and low temperatures, the plasma behaves like a fluid where codes like LASNEX should be able to model accurately. The plasma shifts into a collisionless region with increasing temperature and reducing density, where we expect to observe significant plasma interpenetration.

The target was backlit edge-on by the x-ray laser beam 1.2 ns after the start of the laser pulse that generated the Au plasma. Fig. 1(b) shows the view in the direction of the collimated x-ray laser probe beam which was several millimeters in extend. In Fig. 2 we show the measured interferogram of the colliding plasma with excellent fringe visibility. Near the symmetry axis of the two slabs we observe significantly greater fringe shifts as the results of the plasma collision and subsequent stagnation. The visibility is poorer at the right hand edge of the interferogram due to slight miss-timing in sweeping of the gated detector. We also observed some self emission from the plasma near the slab surface.

At the extreme left and right of the interferogram we can still see the unperturbed fringe pattern where there is no plasma. From these unperturbed fringes, we measure the amount of fringe shift at any position due to the presence of plasma. The beamsplitters were not perfectly flat and that results in one of our experimental uncertainties. Based on previous null shots with similar quality beamsplitters, we estimate the uncertainty to be of order 0.1 fringe. Another source of the uncertainty is the path length across the target plasma in the direction of the collimated x-ray laser beam can be significant since plasma expands in 3-D. [13] In this paper we assume a uniform plasma with a 500 μm path length, which is the transverse width of the optical laser line focus onto the Au slabs.

A motivation to perform the colliding plasma experiment is to examine the validity of LASNEX in a regime that might deviate from the fluid behavior. Fig. 3 shows a snapshot of a LASNEX-calculated 2-D n_e profile at 150 ps after the end of a 1-ns-long, temporally squared optical laser pulse, which corresponds to the peak of the x-ray laser pulse. In this calculation we use a multi-group radiation diffusion method to account for

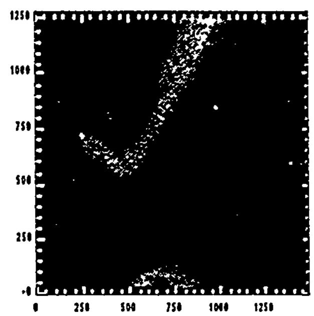

Fig. 2. Measured interferogram of the colliding plasma with excellent fringe visibility and strong self emission near the slab surface. Large fringe shifts on-axis is evident due to plasma stagnation.

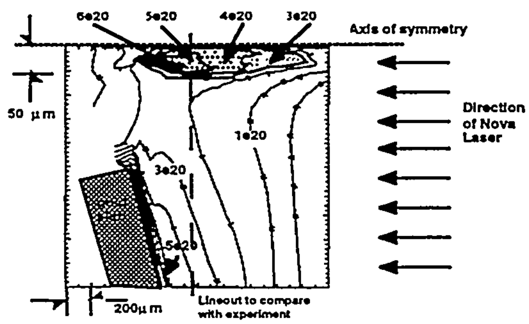

Fig. 3 A snapshot of a LASNEX-calculated 2-D n_e profile at a time of 150 ps after optical laser pulse. This time corresponds to the peak of the x-ray laser pulse that served as the gate for our imaging detector used for the experiment.

the radiative effect. Neglecting the radiation opacity results in significantly lower plasma temperatures. In the blowoff plasma, T_e is as high as 3 keV. Using the three temperature (T_e, T_i, and T_r, the radiation temperature) approximation where the radiation is assumed to be optically thin, LASNEX predicts a T_e of order 0.5 keV. The change in the plasma parameters significantly impact the ionization balance and collisionality of the plasma.

The LASNEX symmetry axis has a mirror reflectivity boundary condition. This geometry simulates the lower half of the experiment. As the blowoff plasma reaches the symmetry axis, the velocity of the zone boundary for a Lagrangian code is set equal to zero, and the slowing and stagnation of the counter-streaming single-fluid plasmas results in the conversion of kinetic to internal energy. In this case T_i can reach a unphysically large values exceeding 10^3 keV. The resulting shock waves, whose intensity depends on the collisionality of the plasma, propagate away from the symmetry axis.

Fig. 4 is a plot of 1-D cuts of the measured and calculated 2-D n_e profiles at 250 µm from the slab tip (at the minimum gap position). The position of this line out is indicated in Fig. 3 and x ~ 800 µm in Fig. 2. Here we observed significant density increase on-axis due to the collision with the measured n_e (solid line) as high as 6 x 10^{20} cm^{-3}. The observed stagnation region has a width of order 100 µm. Although LASNEX (dash-dotted line) predicts a comparable stagnation width, the n_e profile peaks at ~ 30 µm off the symmetry axis and is very characteristic of the shock heated expansion predicted by LASNEX. In the collisionless regime where the plasma is hot and at low densities, n_e will just be the superpositioned density profiles from the two interpenetrating counter-streaming plasmas. The dashed line in Fig. 3 represents a calculated n_e profile of two interpenetrating collisionless plasma streams. At the symmetry plane the measured n_e is a factor of 3-4 higher than the n_e value in the collisionless regime The measured n_e profile falls in between the two calculated n_e profiles, representing the extremes of plasma collisionality. Incorporating plasma interpenetration in our predictive codes, such as multi-specie fluid codes [14,15] should significantly improve our predictive capability of laser-produced plasmas in a colliding configuration.

3. Summary

We have conducted a set of soft x-ray interferometry experiments to study the collision of

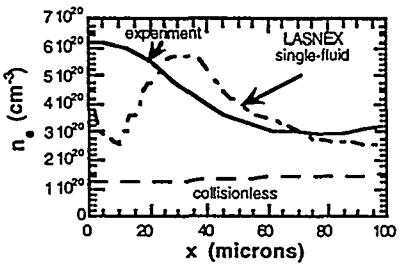

Fig. 4 Comparisons of measured (solid line) and calculated 1-D n_e profiles: LASNEX-calculated single-fluid profile (dashed-dotted line) and profile with a collisionless approximation (dashed line).

high-density, high-temperature plasmas that is of interest to the design of ICF hohlraums. The measured n_e profile peaks at the symmetry plane between the two slabs with a wide stagnation region. The peaked n_e values are a factor of 3-4 larger than the values produced by LASNEX in a collisionless approximation which assumes completely interpenetrating plasmas. Single fluid radiation Lagrangian hydrodynamics codes, such as LASNEX, do not allow for plasma interpenetration and predicts a unphysically large ion temperature and strong shocks propagating from the symmetry plane. The LASNEX-calculated n_e profile, in the signal fluid approximation, shows comparable stagnation width but with n_e profiles peaking off the symmetry plane, which is characteristic of strongly shock-heated, outward propagating plasmas.

The ultimate motivation of the development of soft x-ray laser interferometry is to provide a mechanism to probe the deficiencies of our numerical model in areas such as laser deposition by both resonance and inverse bremsstrahlung absorption, flux-limited heat conduction, hydrodynamics, and non-local thermodynamics equilibrium atomic kinetics. The validation and benchmarking of the codes will allow us to gain better understanding of the physics of high-density laser-produced plasmas as we design more and more complex laser experiments for studying high-energy-density physics, and more specifically for hohlraum and capsule designs for ICF applications.

Acknowledgments

Work performed under the auspices of the U. S. DOE by LLNL under the contract number W-7405-ENG-48 and is partially supported by the Institute Sponsored Research Program.

References

1. S. W. Haan *et al.*, *Phys. Plasmas* 2, 2480–2487 (1995).
2. G. B. Zimmerman and W. L. Kruer, *Com. Plas. Phys. and Cont. Fusion* 2, 51 (1975).
3. L. V. Powers *et al.*, *Phys. Plas.* 2, 2473 (1995); L. V. Powers *et al.*, *Phys. Rev. Lett.* 74, 2957 (1995).
4. D. H. Kalantar *et al.*, *Phys. Plasmas* 2, 3161 – 3168 (1995).
5. J. Lindl, *Phys. Plasmas* 2, 3933 (1995).
6. W. J. Krauser *et al.*, to be published in *Phys. Plasmas*.
7. R. S. Bosch *et al.*, *Phys. Fluids B* 4, 979 – 987 (1992).
8. R. L. Berger *et al.*, *Phys. Fluids B* 3, 3 (1991).
9. O. Larroche, *Phys. Fluids B* 5, 2816 (1993).
10. M. Wilke *et al.*, to appear in "Appl. Laser Plas. Rad. II," SPIE Proc. **2523** (1995).
11. O. Rancu *et al.*, *Phys. Rev. Lett.* 75 3854-3857 (1995).
12. L. B. Da Silva *et al.*, *Phys. Rev. Lett.* 74, 3991 (1995).
13. A. S. Wan *et al.*, *J. Optical Society of America B* 13, 447–453 (1996).
14. P. W. Rambo, J. Denavit, *Phys. Plasmas* 1, 4050–4060 (1994).
15. P. W. Rambo, R. J. Procassini, *Phys. Plasmas* 2, 3130–3145 (1995).

Technical Information Department • Lawrence Livermore National Laboratory
University of California • Livermore, California 94551